Origin of Enantioselectivities in Chiral β-Amino Alcohol Catalyzed Asymmetric Additions of Organozinc Reagents to Benzaldehyde: PM3 Transition State Modeling

Bernd Goldfuss and K. N. Houk*

Department of Chemistry and Biochemistry, University of California, Los Angeles, California 90095-1569

Received July 14, 1998

PM3 transition state (TS) models were developed for enantioselective chiral β-amino alcohol catalyzed additions of organozinc reagents to benzaldehyde. These semiempirical TS models are consistent with earlier ab initio computations on smaller model systems and with experimental data for a variety of stereoselective examples. General trends for varying chiral β-amino alcohol ligands (e.g., camphor, 1,2-diphenylethane, and proline derivatives) and alkylating agent ($ZnMe_2$, $ZnEt_2$) are reproduced by these models.

Introduction

The enantioselective formation of C−C bonds is one of the most important types of synthetic procedures.[1] The additions of organozinc reagents[2] to aldehydes in the presence of small amounts of chiral ligands (L*) are among the most successful catalytic reactions of this type (eq 1).[3]

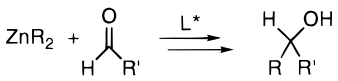

(1)

A number of elegant investigations in the 1980s established the broad utility of this reaction. The first studies of organozinc additions to aldehydes promoted by chiral ligands were carried out by Oguni et al.[4] The Noyori group found that **(−)-1**[5] is especially effective and discovered that the reaction required "two zinc species per aldehyde".[6] Cinchona alkaloids, such as quinine,

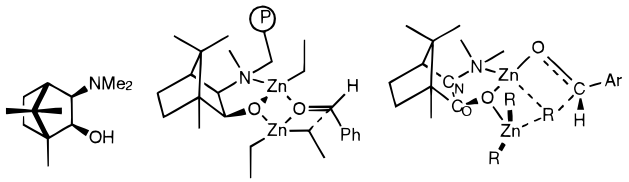

(-)-1 **2** (μ-O TS) **3** (μ-R TS)

were employed as catalysts by Smaardijk et al.,[7] while Itsuno and Fréchet used polymer-bound chiral β-amino alcohols as catalysts.[8] They proposed a transition state model involving two zinc centers bridged by the aldehyde oxygen. This transition state model (μ-O, **2**) is shown for the reaction of diethylzinc with benzaldehyde using a polymer-bound derivative of **1** as chiral ligand.[8]

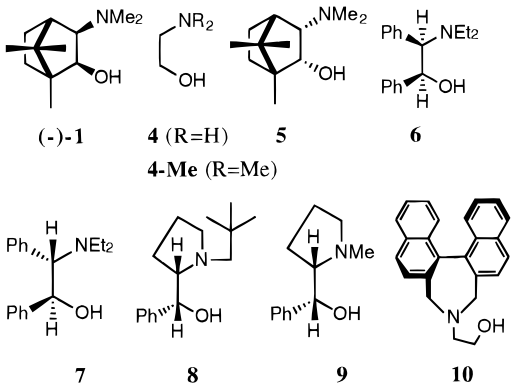

(-)-1 **4** (R=H) **5** **6**
4-Me (R=Me)
7 **8** **9** **10**

Figure 1. Amino alcohol promoters for reactions of organozincs with aldehydes.

The Noyori group postulated an alternative transition state for the addition of $ZnMe_2$ to benzaldehyde catalyzed by **(−)-1**, involving bridging of alkyl groups (μ-R, **3**).[9] This transition state model **3**[10] is in agreement with the experimental observations that the configuration of $C_{(O)}$ primarily determines the stereoselectivity of the β-amino alcohol catayzed reactions.[9]

Evans[3d] and Corey[11] proposed **2a** as transition structure for the **(−)-1** catalyzed addition of diethyl zinc to benzaldehyde.

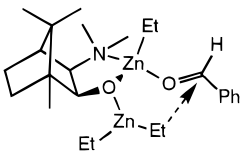

2a

Besides β-amino alcohol camphor derivatives, a huge variety of other ligands and catalysts has been developed

(1) (a) Helmchen, G., Hoffmann, R. W., Mulzer, J., Schaumann, E., Eds.; *Methods of Organic Chemistry* (Houben-Weyl); Thieme: Stuttgart, 1996; Vol. E21. (b) Nógrádi; *Stereoselective Synthesis*; VCH: Weinheim, 1995.

(2) For a recent review on organozinc reagents, see: Knochel, P.; Langer, F.; Longeau, A.; Rottländer, M.; Stüdemann, T. *Chem. Ber./ Recueil* **1997**, *130*, 1021.

(3) For reviews, see: (a) Soai, K.; Niwa, S. *Chem. Rev.* **1992**, *92*, 833. (b) Noyori, R.; Kitamura, M. *Angew. Chem.* **1991**, *103*, 34; *Angew. Chem., Int. Ed. Engl.* **1991**, *30*, 49. (c) Noyori, R. *Asymmetric Catalysis in Organic Synthesis*; Wiley: New York, 1994; p 255. (d) Evans, D. A. *Science* **1988**, *240*, 420.

(4) (a) Oguni, N.; Omi, T.; Yamamoto, Y.; Nakamura, A. *Chem. Lett.* **1983**, 841. (b) Oguni, N.; Omi, T. *Tetrahedron Lett.* **1984**, *25*, 2823.

(5) Chittenden, R. A.; Cooper, C. H. *J. Chem. Soc. C* **1970**, 49.

(6) Kitamura, M.; Suga, S.; Kawai, K.; Noyori, R. *J. Am. Chem. Soc.* **1986**, *108*, 6071.

(7) Smaardijk, A. A.; Wynberg, H. *J. Org. Chem.* **1987**, *52*, 135.

(8) Itsuno, S.; Fréchet, J. M. J. J. *Org. Chem.* **1987**, *52*, 4142.

(9) Kitamura, M.; Okada, S.; Suga, S.; Noyori, R. *J. Am. Chem. Soc.* **1989**, *111*, 4028.

10.1021/jo9813787 CCC: $15.00
Published on Web 11/10/1998

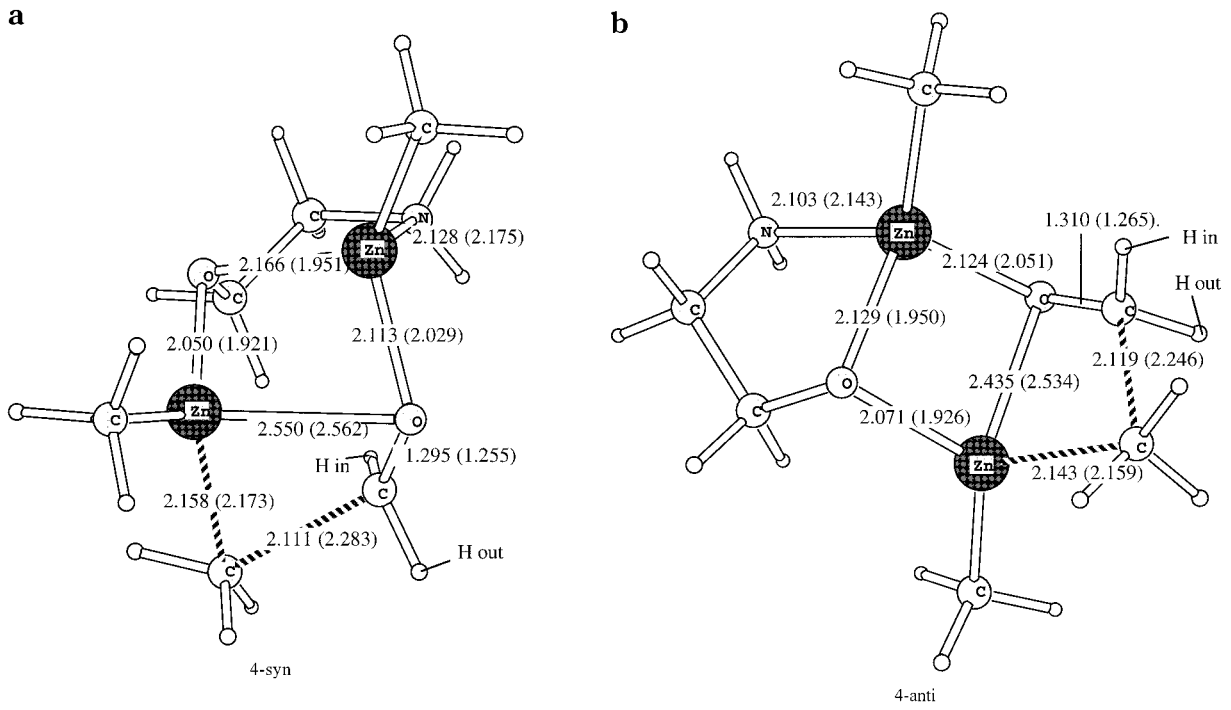

Figure 2. (a) PM3 transition structure **4-syn**. (b) PM3 transition structure **4-anti**. Bond distances in angstroms, (ab initio results are in parentheses).

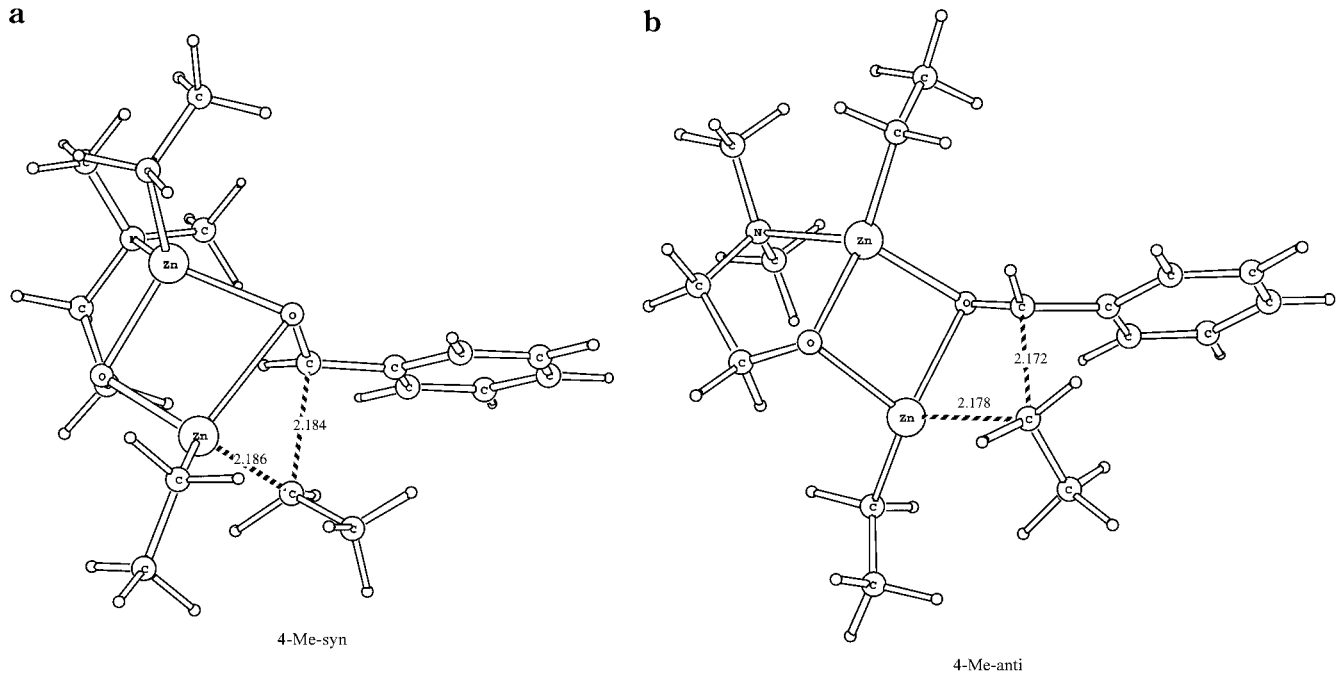

Figure 3. (a) PM3 transition structure **4-Me-syn**. (b) PM3 transition structure **4-Me-anti**. Bond distances are in angstroms.

and applied for this type of reaction, e.g., Soai's proline ligands,[12] Seebach's titanium tetraaryl-1,3-dioxolane-4,5-dimethanolates (TADDOLs),[13] Corey's[11] and Soai's[14] ephedrine derivatives, and Bolm's bipyridines.[15] Organozinc additions to aldehydes promoted by chiral auxiliaries have been employed in the syntheses of an α-tocopherol precurser[16] and an insecticide.[17]

(10) For the related ab initio transition structure in the reaction of methyllithium dimer and formaldehyde, see: Kaufmann, E.; Schleyer, P. v. R.; Houk, K. N.; Wu, Y.-D. *J. Am. Chem. Soc.* **1985**, *107*, 5560.

(11) (a) Corey, E. J.; Hannon, F. J. *Tetrahedron Lett.* **1987**, *28*, 5233. (b) Corey, E. J.; Hannon, F. J. *Tetrahedron Lett.* **1987**, *28*, 5237.

(12) (a) Soai, K.; Ookawa, A.; Ogawa, K.; Kaba, T. J. *Chem. Soc., Chem. Commun.* **1987**, 467. (b) Soai, K.; Ookawa, A.; Kaba, T.; Ogawa, K. *J. Am. Chem. Soc.* **1987**, *109*, 7111.

(13) (a) Schmidt, B.; Seebach, D. *Angew. Chem., Int. Ed. Engl.* **1991**, *30*, 99. (b) Ito, Y. N.; Ariza, X.; Beck, A. K.; Bohac, A.; Ganter, C.; Gawley, R. E.; Kühnle, F. N. M.; Tuleja, J.; Wang, Y. M.; Seebach, D. *Helv. Chim. Acta* **1994**, *77*, 2071.

(14) Soai, K.; Yokoyama, S.; Hayasaka, T. *J. Org. Chem.* **1991**, *56*, 4264.

(15) Bolm, C.; Zhender, M.; Bur, D. *Angew. Chem., Int. Ed. Engl.* **1990**, *29*, 205.

(16) Hübscher, J.; Barner, R. *Helv. Chim. Acta* **1990**, *73*, 1068.

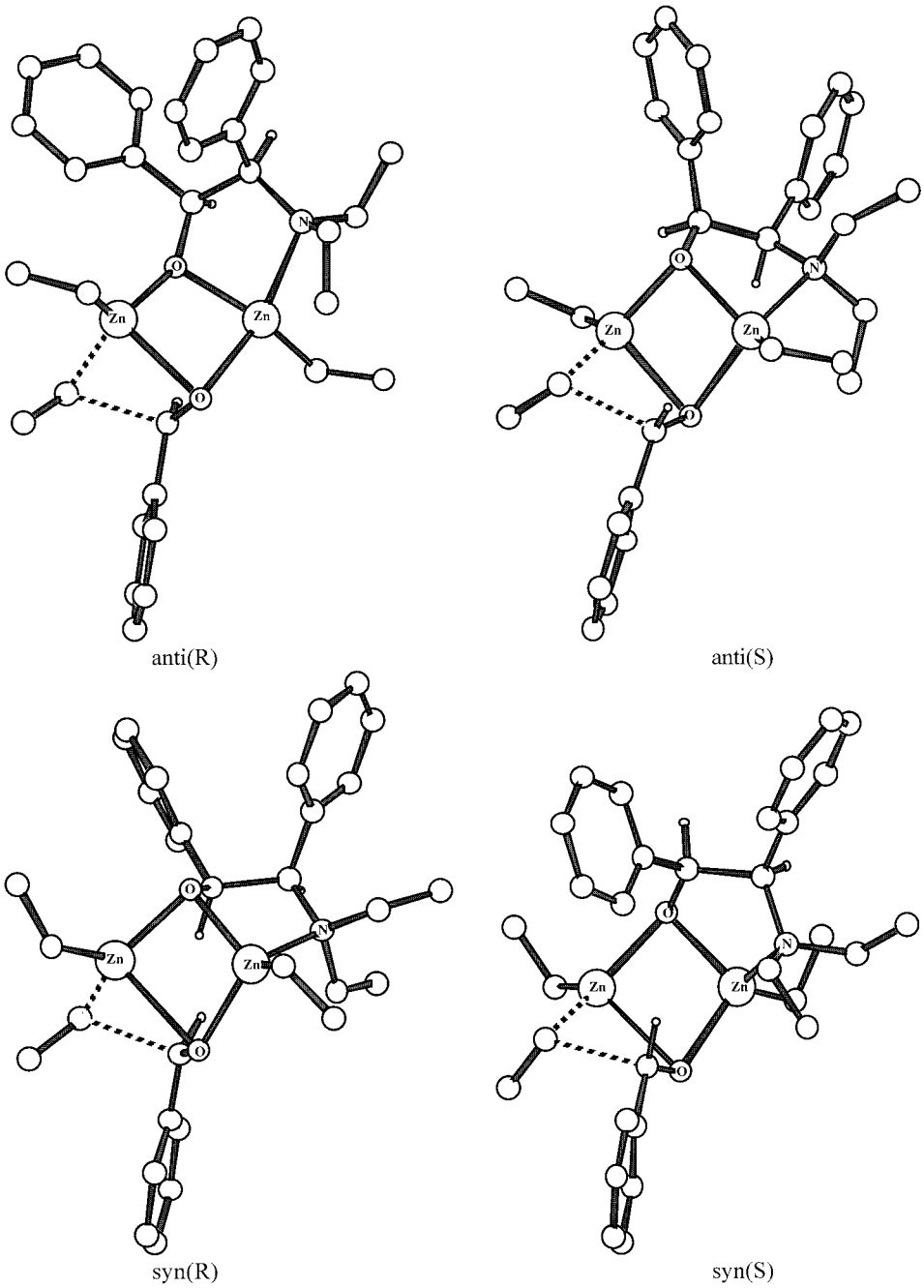

Figure 4. PM3 transition structures based on ligand **6**. Hydrogen atoms are omitted for clarity, except for stereocenters, in Figures 4−10.

In a previous theoretical study of the mechanism of the reaction, Yamakawa and Noyori used MP2//HF ab initio methods to compute the transition structures with a $H_2N(CH_2)_2OH$ (**4**) ligand in a model reaction between $ZnMe_2$ and formaldehyde. Two low energy μ-O transition structures, **4-syn** and **4-anti**, were located,[18] but no μ-R structures, as shown in **3**, were found.

Recently, Vidal-Ferran et al. used these ab initio geometries combined with AM1 optimizations for a computer-assisted ligand design to study enantioselectivities in diethyl zinc additions to aldehydes.[19]

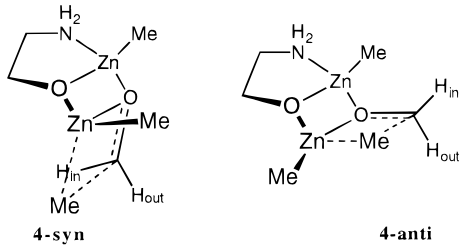

We have undertaken a computational investigation of the origin of stereoselectivities in these dialkyl zinc additions. We have previously developed force field transition state models for the exploration of stereoselectivity of a variety of reactions.[20] Because of the labor involved in the development of force field parameters, we

(17) Tombo, G. M. R.; Didier, E.; Loubinoux, B. *Synlett* **1990**, 547.
(18) Yamakawa, M.; Noyori, R. *J. Am. Chem. Soc.* **1995**, *117*, 6327.
(19) AM1 optimized residues on a fixed core-geometry were used: Vidal-Ferran, A.; Moyano, A.; Pericàs, M. A.; Riera, A. *Tetrahedron Lett.* **1997**, *38*, 8773.

Table 1. Relative Heats of Formation (ΔH_f, kcal/mol)[a] and Computed Ratios of (*S*) and (*R*) Enantiomers (*S*:*R*)[b] of the Alcoholic Products for PM3 Transition Structures Based on Chiral β-Amino Alcohol Ligands (Figure 1), O=CHPh, and $ZnEt_2$ ($ZnMe_2$)

	1	**5**	**6**	**7**	**8**	**9**	**10**
syn(R)-a	−1.3 (0)[d]	*c*	−0.9	−1.4	13.1	12.0	2.3
syn(R)-b	−0.7		−0.7	−1.1	13.5	12.3	2.4
syn(R)-c	−0.6		−0.4	−0.3	14.3	12.4	3.0
syn(R)-d	0		0	0	14.9	13.7	4.4
anti(S)-a	−4.8 (−2.4)[d]		−5.0	−3.9	2.7	4.1	−0.9
anti(S)-b	−4.2		−4.7	−3.7	3.0	4.50	−0.6
anti(S)-c	−3.6		−4.4	−3.6	4.4	5.9	−0.5
anti(S)-d	−3.1		−4.3	−3.5	5.4	6.6	0
syn(S)-a	*c*	−1.9	10.7	4.2	−0.8	−0.2	3.0
syn(S)-b		−1.6	10.8	6.0	−0.3	−0.2	3.5
syn(S)-c		−0.7	10.9	6.4	−0.0	−0.2	5.1
syn(S)-d		0	11.0	6.4	0	0	5.7
anti(R)-a		−4.9	5.1	−0.7	−2.9	−1.7	−0.3
anti(R)-b		−4.9	5.2	−0.3	−2.8	−1.6	−0.3
anti(R)-c		−4.8	5.6	5.9	−2.6	−1.2	−0.1
anti(R)-d		−3.9	7.1	6.4	−2.4	−0.8	−0.1
S:*R*	530:1 (87:1)[d]	1:440	1800:1	120:1	1:72	1:10	2:1

[a] TS **-a** to **-d** represent transition structures with different ethyl group conformations; the imaginary frequencies are at ∼−500 cm^{-1}; zero point energies are included. [b] Configuration of formed alcohol; $T = 273.15$ K, $R = 1.986$ cal K^{-1} mol^{-1}. [c] No transition structures were found for this coordination mode. [d] $ZnMe_2$ as alkylating reagent.

have explored here the alternative of semiempirical methods for the investigation of stereoselectivities in these reactions. Successful stereochemical applications of semiempirical methods to related reactions were reported previously: 2-azanorbornylmethanethiol-catalyzed diethyl zinc additions to aldehydes (PM3)[21] and oxazaborolidine-catalyzed reductions of ketones (MNDO).[22]

We first validated PM3 transition state geometries for this reaction, by careful comparison of results on model systems with those obtained from ab initio methods. We then explored the transition states of reactions with the ligands **1** and **5**−**10** (Figure 1) and compared the results with experimental data.

The successful use of semiempirical techniques for stereoselectivity modeling requires only that the relative energies of diastereomeric transition states be accurate. The more demanding prediction of absolute activation energies is not necessary. We show that this method gives a practical tool for stereoselection predictions and has led us to a quantitative model which explains the origin of selectivity in these reactions.

Results and Discussion

We first tested whether PM3 correctly reproduces previous ab initio geometries and energies for the model systems **4-syn** and **4-anti**. The geometries of the PM3 transition structures **4-syn** and **4-anti** are compared to those obtained from RHF/3-21G (C, H, N, O); /[8s4p2d] (14s9p5d) (Zn) calculations in Figure 2. The Zn−O contacts are computed ca. 0.1 Å longer and Zn−N bonds somewhat shorter by the PM3 method, but ab initio and PM3 methods are in reasonable agreement about the geometries of the reaction centers (Figure 2). The ab initio RMP2//RHF calculations predict that **4-anti** is 2.9 kcal/mol more stable than **4-syn**, while the PM3 transition structures predict a 6.8 kcal/mol difference. The transition structures for the reaction of $ZnEt_2$ with benzaldehyde with the $Me_2N(CH_2)_2OH$ ligand (**4-Me**, Figure 1) were also computed. The PM3 preference for **4-Me-anti** over **4-Me-syn** is less pronounced (3.6 kcal/mol) than for **4**. The structures of **4-Me** are shown in Figure 3. In both **4-Me-syn** and **4-Me-anti**, the bulky phenyl group of benzaldehyde adopts the less crowded "out" rather than the "in" positions, which were found to be highly unfavorable.[23] On the basis of the similarities in geometries and relative energies of "syn" and "anti" transition structures obtained by PM3 and ab initio RHF

Table 2. Computed ($\%ee_{comp}$) and Experimental ($\%ee_{exp}$) Enantioselectivities for Chiral Amino Alcohol Catalyzed Reactions of Organozinc Reagents with Benzaldehyde[a]

TS	$ratio_{comp}$[b]	$config_{comp}$	$\%ee_{comp}$[c]	$\%ee_{exp}$ (config)
(−)-1 ($ZnEt_2$)	530:1	(*S*)	100	99 (*S*)
(−)-1 ($ZnMe_2$)	87:1	(*S*)	98	91 (*S*)
(+)-1 ($ZnEt_2$)	530:1	(*R*)	100	98 (*R*)
5 ($ZnEt_2$)	440:1	(*R*)	99	95 (*R*)
6 ($ZnEt_2$)	1800:1	(*S*)	100	94 (*S*)
7 ($ZnEt_2$)	120:1	(*S*)	98	81 (*S*)
8 ($ZnEt_2$)	72:1	(*R*)	97	100 (*R*)
9 ($ZnEt_2$)	10:1	(*R*)	82	72 (*R*)
10 ($ZnEt_2$)	2:1	(*S*)	33	49 (*S*)

[a] See Table 1 for relative energies. [b] $T = 273.15$ K, $R = 1.986$ cal K^{-1} mol^{-1}.

(20) Eksterowicz, J. E.; Houk K. N. *Chem. Rev.* **1993**, *93*, 2439.

(21) Nakano, H.; Kumagai, N.; Matsuzaki, H.; Kabuto, C.; Hongo, H. *Tetrahedron: Asymmetry* **1997**, *8*, 1391. The activation energy of the reaction (∼14 kcal/mol) and the energy difference between (*R*)- and (*S*)-TS (3.6 kcal/mol) were computed, but no detailed descriptions of the transition structures were given.

(22) Jones, D. K.; Liotta, D. C.; Shinkai, I.; Mathre, D. J. *J. Org. Chem.* **1993**, *58*, 799.

(23) The Ph_{in} geometries of μ-O−PM3 transition structures were highly disfavored both for syn and anti structures due to strong steric repulsions. These unfavorable interactions arise for syn structures from close distances between the Ph_{in} groups and the zinc chelate ring and for the anti structures from close distances between the Phin groups and the alkyl groups (R) attached to zinc:

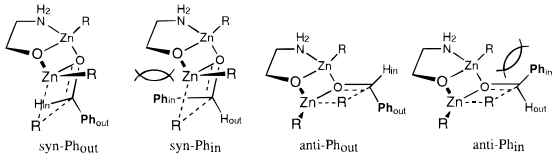

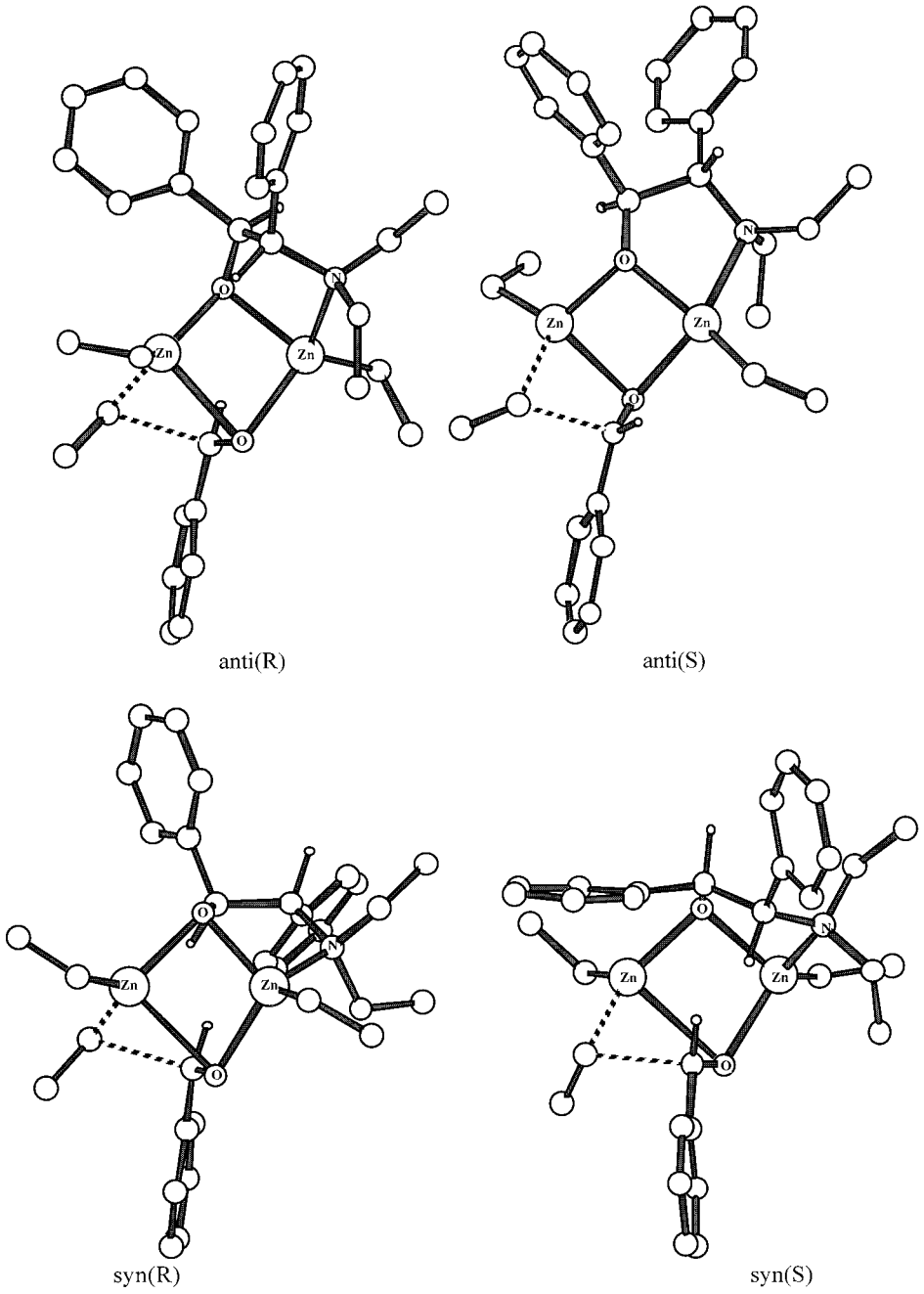

Figure 5. PM3 transition structures based on ligand **7**.

calculations, we have tested PM3 for a variety of organozinc additions involving chiral ligands.

Four μ-O transition structure types with "syn" and "anti" geometries yielding each (*R*)- and (*S*)-alcoholic products are possible for the chiral β-amino alcohols **1** and **5**−**10** (Figure 1). Transition structures based on (1*R*,2*S*)-2-(diethylamino)-1,2-diphenylethanol (**6**),[24] exhibit all possible combinations: **anti(R)**, **anti(S)**, **syn-(R)**, and **syn(S)** (Figure 4). For each of these four possible "syn", "anti" and *R*,*S* combinations, four transition structures were computed (**-a** to **-d**, Table 1) to account for conformational flexibilities. The transition structures (**-a** to **-d**) represent the four most stable geometries, which were found by rotating around Zn−Et and N−Et bonds in 30° steps and subsequent transition state reoptimization. The most stable structures (**-a**) are shown in the figures. The **anti(S)** and **syn(R)** transition structures are most stable for ligand **6** (Table 1). Figure 4 shows that these more stable **6-anti(S)** and **6-syn(R)** transition structures result from aldehyde coordinations at the less hindered face of the Zn(O−CPh−CPh−N) five-membered chelate ring: both phenyl groups of the ligand are trans to the coordinated aldehyde and the $ZnEt_2$ moieties in **6-anti(S)** and **6-syn(R)**. In contrast, **6-anti(R)** and **6-syn(S)** are much higher in energy (Table 1) due to less favorable syn alignments of the ligand phenyl groups and the coordinated aldehyde and $ZnEt_2$ moieties (Figure 4). The energy differences between the more stable **6-anti(S)** and **6-syn(R)** struc-

(24) Noyori, R.; Suga, S.; Kawai, K.; Okada, S.; Kitamura, M.; Oguni, N.; Hayashi, M.; Kaneko, T.; Matsuda, Y. *J. Organomet. Chem.* **1990**, *382*, 19.

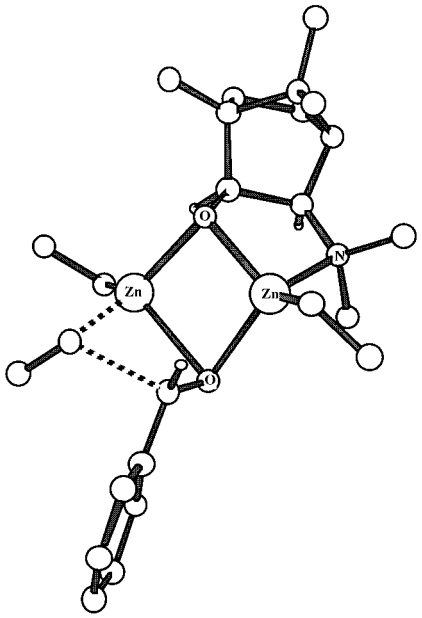

anti(S)

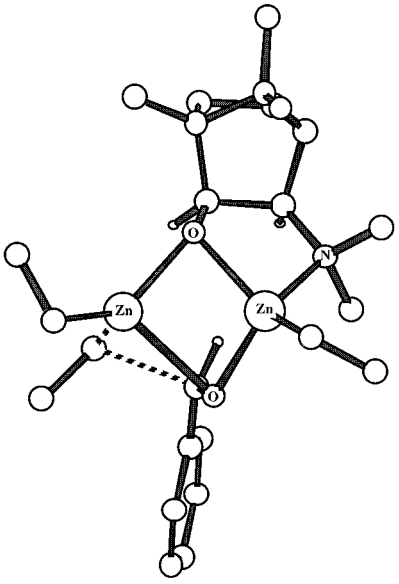

syn(R)

Figure 6. PM3 transition structures based on ligand **1**.

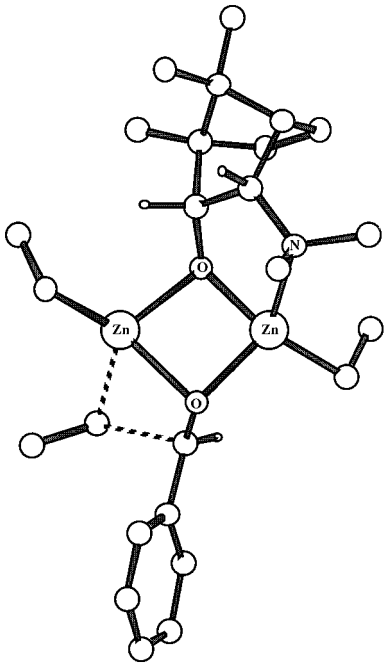

anti(R)

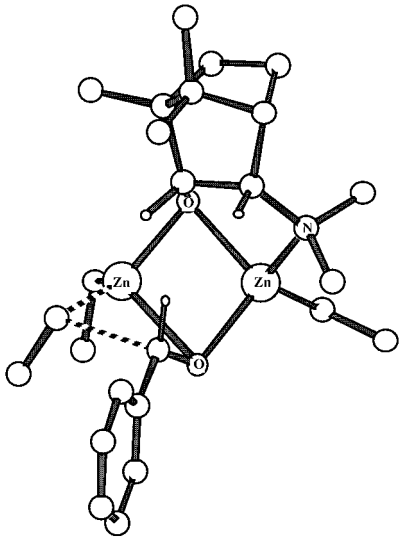

syn(S)

Figure 7. PM3 transition structures based on ligand **5**.

tures account for enantioselectivity in favor of the (*S*)-alcoholic product (*S*:*R* = 1800:1, Table 1), which is in agreement with experimental results (Table 2).

The change of the configuration at $C_{(N)}$ in (1*R*,2*R*)-2-(diethylamino)-1,2-diphenylethanol (**7**) does not change the **anti(S)** < **syn(R)** < **anti(R)** < **syn(S)** (transition structures in Figure 5) energy order relative to **6** (Table 1): the higher stability of **7-anti(S)** transition structures over **7-syn(R)** transition structures results again in the formation of the (*S*)-alcoholic product. The energy differences are, however, smaller between **7-anti(S)** and **7-anti(S)** than between **6-anti(S)** and **6-syn(R)** and result in a decreased enantioselectivity for **7** (*S*:*R* = 120:1, Table 1). The lower enantioselectivity of **7** relative to **6** is in agreement with experiments (Table 2). This supports Noyori's empirical rule that the configuration of $C_{(O)}$ is more important for the stereochemical outcome of the reaction than the configuration of $C_{(N)}$.[3b,c,9]

For the transition structures of the camphor derivatives **1** (Figure 6) and **5** (Figure 7), no species of the **syn-(S)** or the **anti(R)** type could be located (Table 1), since steric hindrance in such species is so large. This accounts for the large stereodiscrimination of the exo camphor skeleton in **1** and of the endo side in **2**.[25] Enantioselection arises from energy differences between **1-anti(S)** and **1-syn(R)** structures for **1** and between **5-anti(R)** and **5-syn(S)** structures for **5**. The ligand **1** yields a higher enantioselectivity (*S*:*R* = 530:1, Table 1) than computed for **5** (*S*:*R* = 1:440, Table 1), which is in agreement with

(25) For a discussion of "exo" and "endo" approaches of nucleophiles to camphor see: Eliel, E. L.; Wilen, S. H.; Mander, L. N. *Stereochemistry of Organic Compounds*; Wiley: New York 1994; p 736.

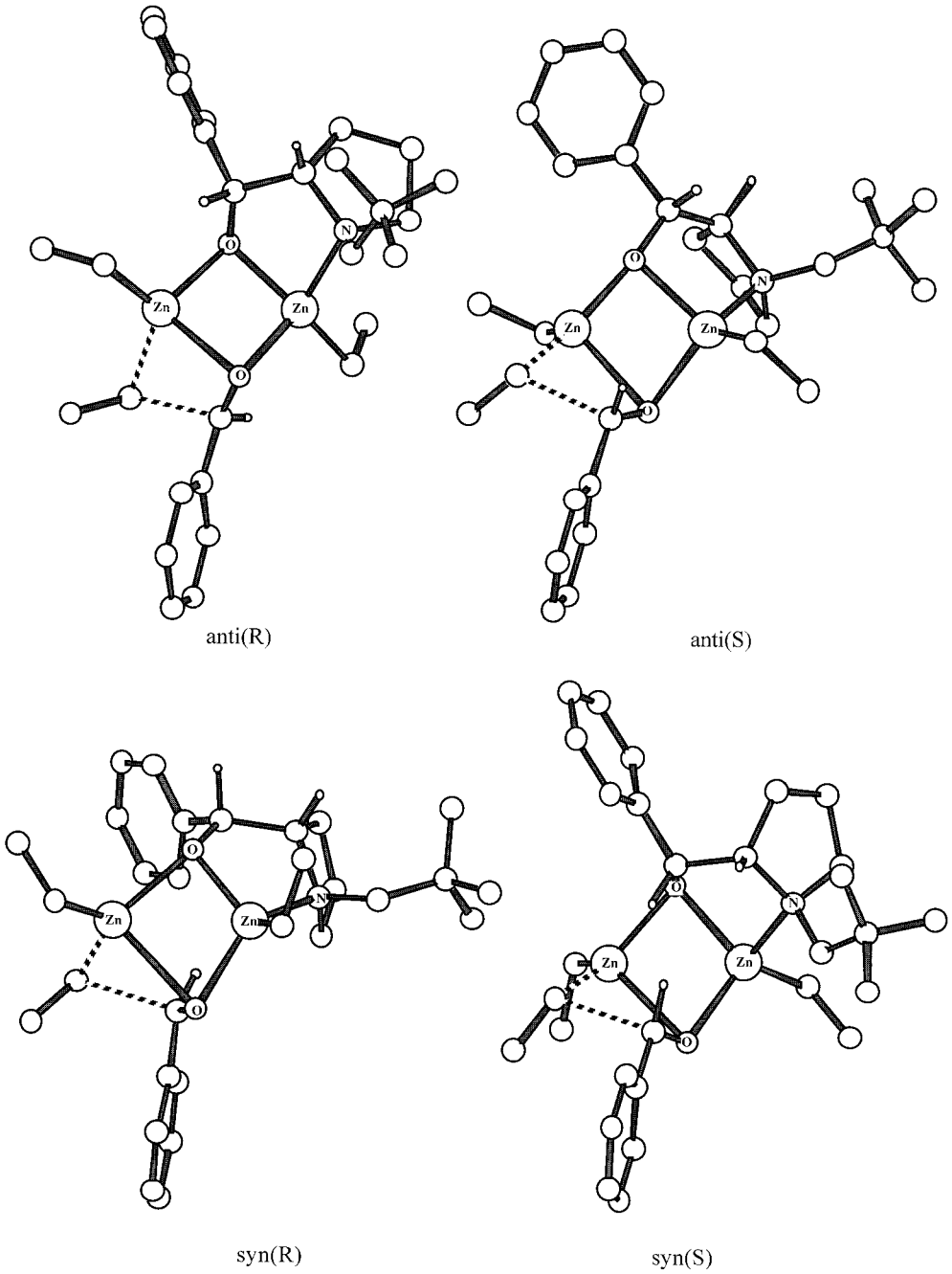

Figure 8. PM3 transition structures based on ligand **8**.

experimental results (Table 2). If $ZnMe_2$ rather than $ZnEt_2$ is employed as alkylating reagent with **1**, the enantioselectivity drops to *S*:*R* = 87:1 (Table 1). This lower enantioselectivity with $ZnMe_2$ also agrees with experimental results (Table 2).

Transition structures with the (*S*)-proline derivatives **8** (Figure 8) and **9** (Figure 9) adopt all four structure types, now with the **anti(R)** < **syn(S)** < **anti(S)** < **syn-(R)** order in relative energy (Table 1). The high relative energies of **anti(S)** and **syn(R)** transition structures are due to the unfavorable syn alignments of the ligand phenyl groups relative to the coordinated aldehyde and $ZnEt_2$ moieties (Figures 8 and 9). The neopentyl substituent at N in **8** results in a higher enantioselectivity (*S*:*R* = 1:72, Table 1) than the methyl (N) substituent in **9** (*S*:*R* = 1:10, Table 1). The higher enantioselectivity of **8** relative to **9** is in agreement with experimental results (Table 2).

The C_2-symmetric binaphthyl substituent at N in **10** gives rise to much lower stereoselectivity than is shown by the other ligands. Transition structures with **10** exhibit an **anti(S)** < **anti(R)** < **syn(R)** < **syn(S)** order of relative energies (Table 1). There are only small energy differences between "syn" and "anti" structures. Figure 10 shows that the binaphthyl substituent at N does not efficiently distinguish the faces of the five-membered Zn-chelate ring. The lack of a substituent at $C_{(O)}$ eliminates significant repulsive interactions with the bulky $ZnEt_2$ moieties (Figure 10). The enantioselectivity results mainly from the small energy differences of **10-anti(S)** and **10-anti(R)** structures and is relatively poor

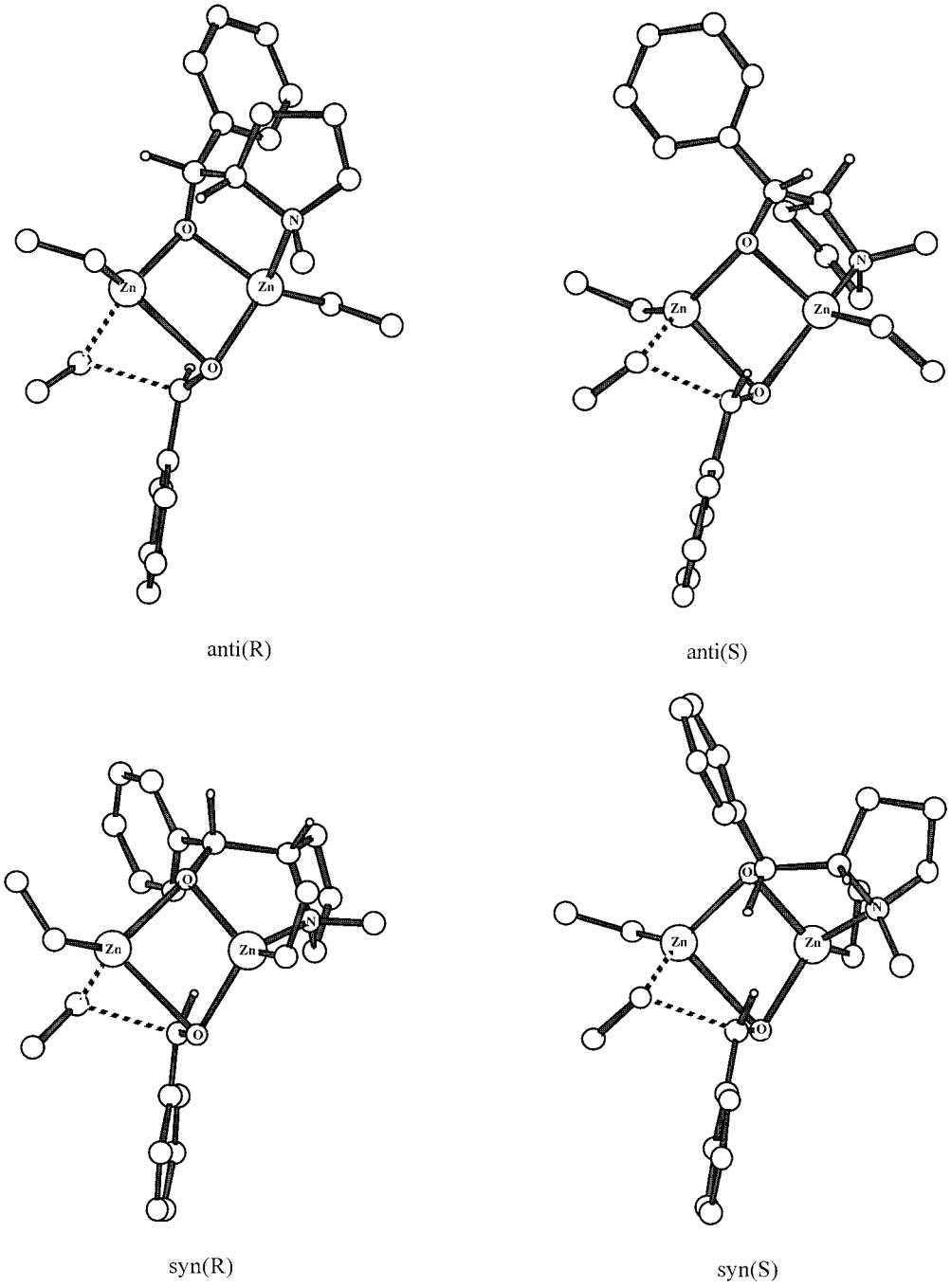

Figure 9. PM3 transition structures based on ligand **9**.

(*S*:*R* = 10:1, Table 1). This low enantioselectivity in favor of the (*S*)-product is in accord with experiments (Table 2).

Conclusions

The PM3 μ-O TS models for chiral β-amino alcohols correctly reproduce the directions and the general trends of enantioselectivity with variations of ligands and different alkylating agents. The high degree of enantioselectivity for the ligands **1** and **5**−**9** arise from energy differences between the most stable "syn" and "anti" transition structures. Substituents at $C_{(O)}$ more efficiently interact with the large ZnR_2 moieties (coordinated to O) than $C_{(N)}$ substituents and are more important determinants of enantioselectivity. The alkyl group transfers from the ZnR_2 moieties to the coordinated aldehydes occur preferentially at the less hindered face (small substituent at $C_{(O)}$) of the five-membered chelate ring. The most stable "anti" structures determine the configurations of the alcoholic products. Structures **11** and **12** summarize the features in the transition structures leading to the major (e.g., (*S*)-alcohol) or minor (e.g., (*R*)-alcohol) products.

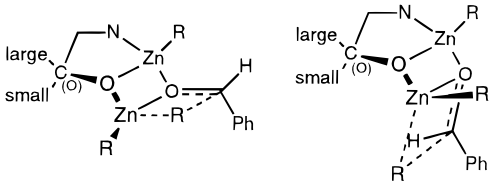

11 (major TS) **12** (minor TS)

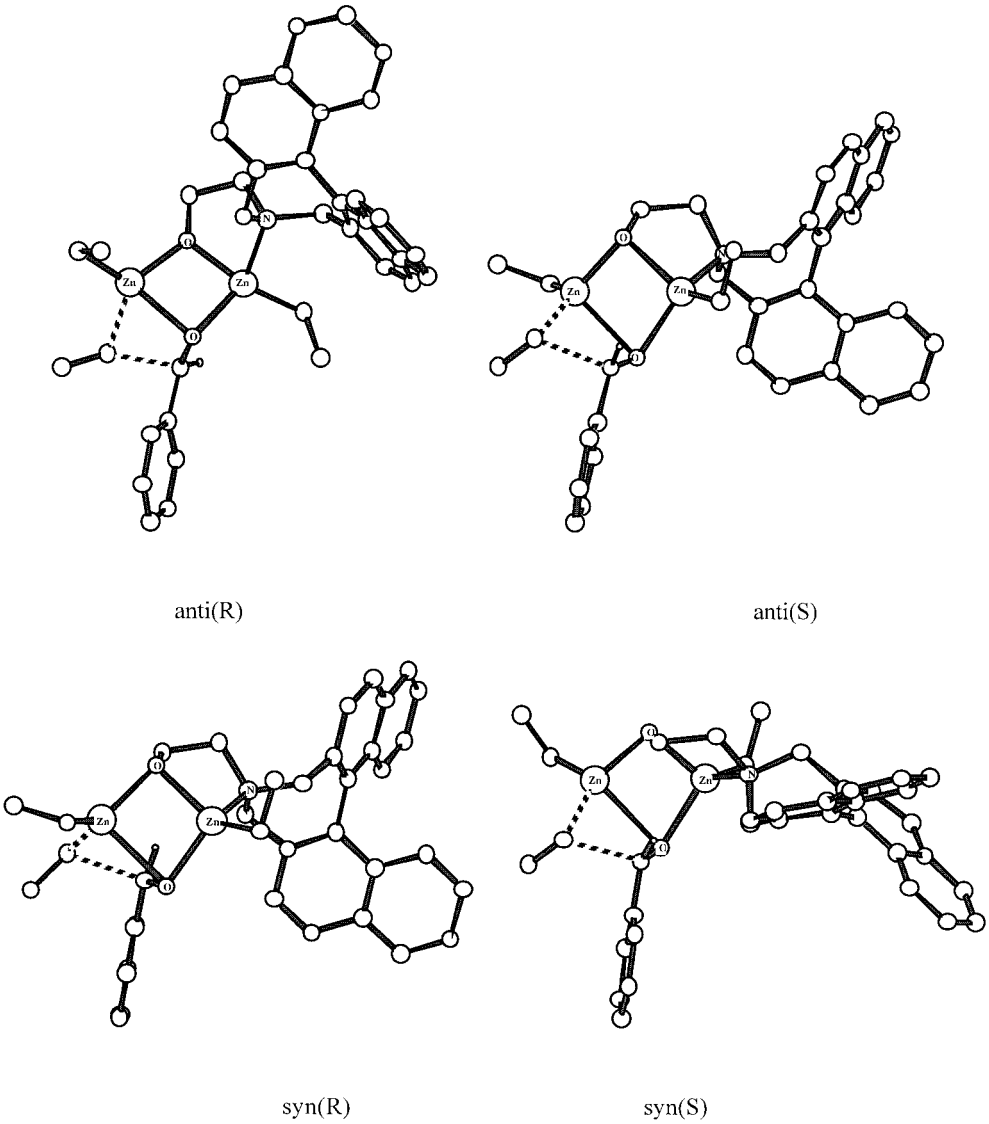

Figure 10. PM3 transition structures based on ligand **10**.

Applications to predictions of new ligands and related reactions with different substrates will be reported in due course.

Computational Methods

All PM3[26] transition structures were fully optimized with Powell's NS01A method,[27] using the program VAMP 6.1.[28] Optimizations and force computations, yielding geometries, zero point energies, and frequencies were processed with increased SCF and gradient norm criteria (PRECISE).

Acknowledgment. We are grateful to the National Institutes of Health for financial support of this work. B.G. thanks the Alexander von Humboldt-Stiftung for a Lynen Fellowship.

JO9813787

(26) For PM3 parameters, see: Stewart, J. J. P. *J. Comput. Chem.* **1989**, *10*, 209, 221; *J. Comput. Chem.* **1991**, *12*, 320.

(27) Powell, M. J. D., Ed.; *Non-Linear Optimization*; Academic Press: New York, 1982.

(28) Rauhut, G.; Alex, A.; Chandrasekhar, J.; Steinke, T.; Sauer, W.; Beck, B.; Hutter, M.; Gedeck, P.; Clark, T., Erlangen 1996.